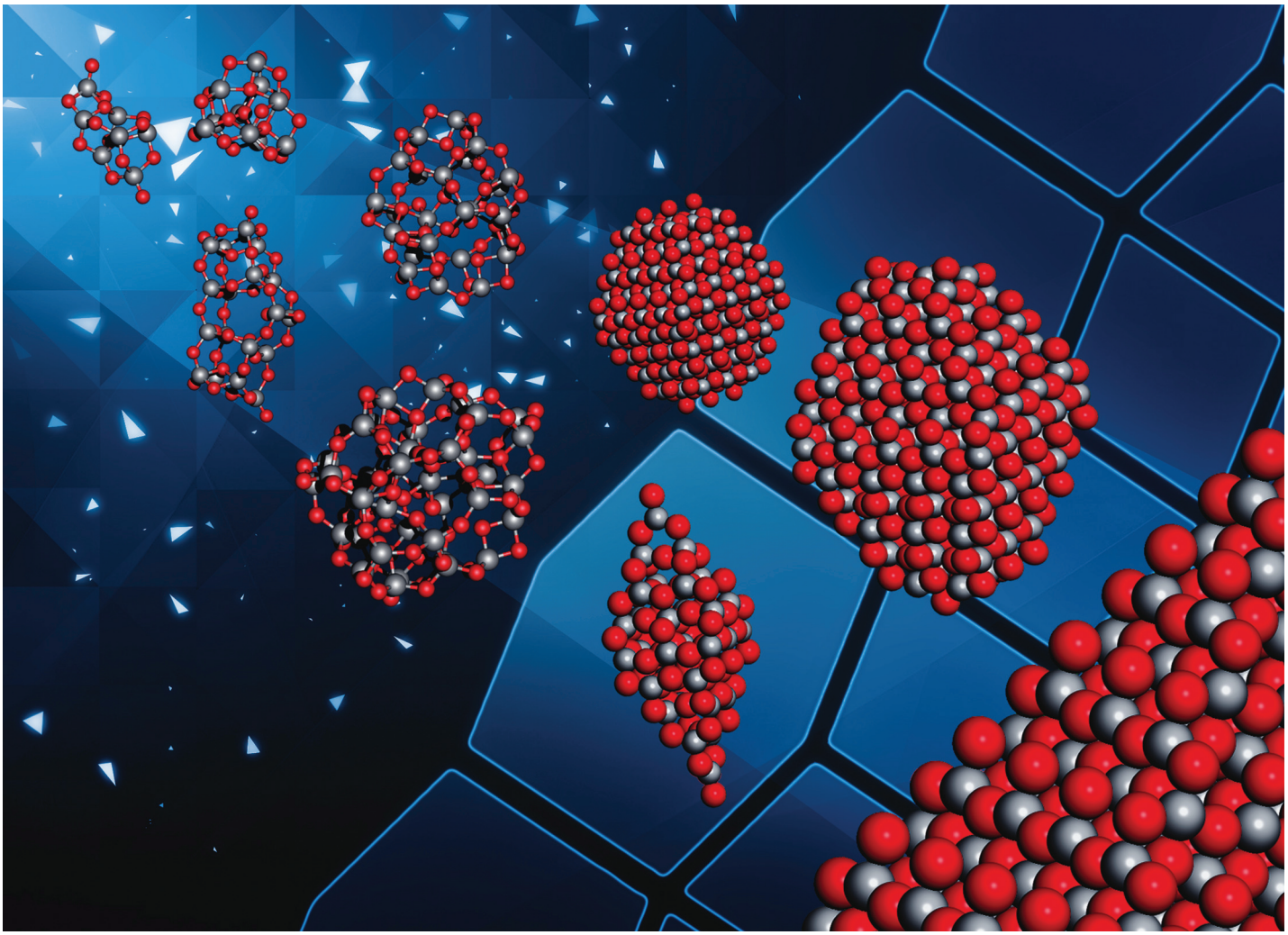

Showcasing research from the group of Stefan Bromley, Nanoclusters and Nanostructured Materials Group, Institute of Computational and Theoretical Chemistry, University of Barcelona, Spain.

Predicting size-dependent emergence of crystallinity in nanomaterials: titania nanoclusters *versus* nanocrystals

Bottom-up and top-down derived nanoparticle structures refined by accurate *ab initio* calculations are used to investigate the size dependent emergence of crystallinity in titania from the monomer upwards. Consistent with available experimental data, we predict to a non-crystalline to crystalline crossover size for nanoparticles with 2–3 nm diameter.

As featured in:

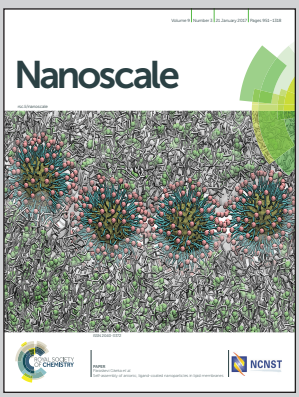

See Stefan T. Bromley *et al.*, *Nanoscale*, 2017, **9**, 1049.

ROYAL SOCIETY OF CHEMISTRY

rsc.li/nanoscale

Registered charity number: 207890

Nanoscale

PAPER

View Article Online
View Journal | View Issue

Cite this: *Nanoscale*, 2017, **9**, 1049

Predicting size-dependent emergence of crystallinity in nanomaterials: titania nanoclusters *versus* nanocrystals†

Oriol Lamiel-Garcia,[a] Andi Cuko,[a,b] Monica Calatayud,[b,c] Francesc Illas[a] and Stefan T. Bromley*[a,d]

Received 22nd July 2016,
Accepted 4th October 2016

DOI: 10.1039/c6nr05788h

www.rsc.org/nanoscale

Bottom-up and top-down derived nanoparticle structures refined by accurate *ab initio* calculations are used to investigate the size dependent emergence of crystallinity in titania from the monomer upwards. Global optimisation and data mining are used to provide a series of $(TiO_2)_N$ global minima candidates in the range $N = 1–38$, where our approach provides many new low energy structures for $N > 10$. A range of nanocrystal cuts from the anatase crystal structure are also considered up to a size of over 250 atoms. All nanocrystals considered are predicted to be metastable with respect to non-crystalline nanoclusters, which has implications with respect to the limitations of the cluster approach to modelling large titania nanosystems. Extrapolating both data sets using a generalised expansion of a top-down derived energy expression for nanoparticles, we obtain an estimate of the non-crystalline to crystalline crossover size for titania. Our results compare well with the available experimental results and imply that anatase-like crystallinity emerges in titania nanoparticles of approximately 2–3 nm diameter.

Introduction

Size reduction from the macroscopic to length scales of only a few nanometres can lead to dramatic changes in a material's properties. Further to the effects directly arising from high surface-to-bulk ratios, nano-sized particles often possess distinct atomic and electronic structures with respect to stable bulk crystals. Titania (TiO_2) is a prototypical example of a material displaying an extreme size-dependence of both structure and properties.[1] Under ambient conditions bulk titania is most thermodynamically stable with atomic ordering following the rutile crystal structure. However, upon reduction in size, titania nanoparticles with average diameters less than ~14 nm begin to exhibit the anatase crystal structure.[2] This structural transition has been thermodynamically rationalised by top-down calculations of the size-dependent enthalpies of titania nanoparticles, which highlight the roles of surface energies and surface stresses on nanoparticle stability.[2,3]

Anatase nanocrystals are found to greatly differ from their rutile counterparts in being highly photochemically active and form the basis for many nano-titania based applications (*e.g.* photocatalysts,[4] sunscreens,[5] anti-pollution building materials[6]). Often the key to enhanced photoactivity is to form composite materials containing very small (≤5 nm diameter) stable anatase nanocrystals.[7,8] As with most materials, however, further decreasing the size of anatase nanocrystals will eventually give way to a regime of nanoclusters, which generally do not display a crystalline order, thus losing much of their utility. Evidence from high resolution transmission electron microscopy has shown that isolated anatase nanocrystals can persist down to sizes as small as ~5 nm in diameter.[9] Recent experiments have further shown that the anatase crystal structure is extremely thermally persistent in 4 nm diameter nanoparticles.[10] Although this implies that anatase is still thermodynamically stable, in this latter size range it is unclear whether such nanoparticles retain a facetted nanocrystal morphology. Indirect evidence from modelling suggests that when anatase nanoparticles start to become smaller than ~5 nm, they may begin to exhibit a spherical morphology with an anatase core and an amorphous shell.[11] Although not strictly nanocrystals according to our definition, such core–shell nanoparticles should clearly be regarded as partially crystalline. For even smaller TiO_2 nanoparticles, with average

[a]*Departament de Ciència de Materials i Química Física and Institut de Química Teòrica i Computacional (IQTCUB), Universitat de Barcelona, E-08028 Barcelona, Spain*
[b]*SorbonneUniversités, UPMC Univ Paris 06, CNRS, Laboratoire de Chimie Théorique CC 137, 4, place Jussieu F. 75252, Paris Cedex 05, France*
[c]*InstitutUniversitaire de France, France*
[d]*Institució Catalana de Recerca i Estudis Avançats (ICREA), E-08010 Barcelona, Spain. E-mail: s.bromley@ub.edu*
†Electronic supplementary information (ESI) available. See DOI: 10.1039/c6nr05788h

diameters in the range 2–3 nm, fitting experimental X-ray spectroscopy data using the reverse Monte Carlo refined nanoparticle structures tend to support this feature.[12] With decreasing size, eventually the anatase core is subsumed by the amorphous shell, and the nanoparticles will not exhibit any crystallinity. We refer to the non-crystalline titania species in this ultra-small size regime as nanoclusters.

From a bottom-up perspective, increasing in size from a single TiO_2 monomer, nanoclusters need to attain a certain size before they begin to thermodynamically favour regular atomic ordering characteristic of a bulk crystal. From this perspective, this structural crossover between nanoclusters and nanocrystals can be seen as a size-dependent non-crystalline to crystalline (NC ↔ C) crossover. Herein, we provide an estimate of the NC ↔ C crossover size regime for TiO_2 using accurate quantum chemically calculated energies of relaxed atomistically detailed nanoclusters and nanocrystals derived from bottom-up and top-down approaches respectively.

In Fig. 1 we represent the generic size dependent energetic stability of both non-crystalline (red line) and nanocrystals (blue line) for an arbitrary material. We note that although herein we will use calculated energies at 0 K to demonstrate our approach, these data could equally well be free energies from experiment and/or theory. The energy difference, $\Delta E_{C-NC}(N)$, gives a measure of the metastability of crystalline particles with respect to non-crystalline clusters at relatively small sizes and *vice versa* at larger sizes. Using the plotted energies the NC ↔ C crossover size would seem to be defined as the size at which $\Delta E_{C-NC}(N)$ becomes zero. In general, however, it is not expected that this crossover will always be defined by a definite single transition size above which nanocrystals are always more energetically stable and below which non-crystalline nanoclusters are always more stable. Size dependent structural preferences are well-known in nanocluster systems (*e.g.* icosahedral shell closing) and it is quite possible that, with increasing size, crystallinity would be first energetically favoured in a set of discrete increasingly sized nanoparticles covering a crossover range (N_1, N_2, ... N_C) before being manifestly prevalent for all $N \geq N_C$. More generally, it is quite likely that for sizes close to but smaller than N_C there will be nanoclusters that exhibit partial crystallinity (*e.g.* a nanoparticle with crystalline cores and an amorphous shell). As such we define the NC size range as those nanoparticles which do not exhibit full crystallinity. In turn, we roughly define a fully crystalline nanocrystal as one which can be cut from a bulk crystal and which maintains its atomic ordering upon structural relaxation and with only minor displacement of atomic positions (*i.e.* no more than a ~20% of a bond length). We further note that the NC ↔ C crossover will not generally be to the most stable bulk crystalline phase of the material but rather to a polymorph which is metastable in the bulk. Depending on the material there will be variable number of subsequent size dependent crossovers between polymorphs until the most stable bulk crystalline phase is reached.

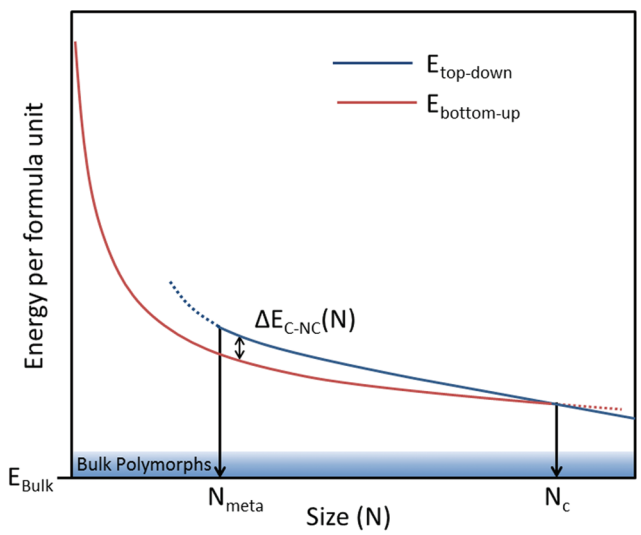

Fig. 1 Schematic representation of size-dependent energetic stability of crystalline (C) and non-crystalline (NC) nanoparticles with respect to their size. The red line indicates the stability of nanoclusters and the blue line that of nanocrystals. $\Delta E_{C-NC}(N)$ denotes the energy difference between a nanocrystal and nanocluster, both having N formula units. The blue shaded region denotes the typical energy range within which metastable bulk polymorphs can exist. N_{meta} and N_C are described in the text.

In Fig. 1 we also note another interesting crossover size, N_{meta}, indicating the smallest size that a nanocrystal can maintain an energetically metastable crystalline structure with respect to a non-crystalline nanocluster of the same size. Related to this concept, there have been important studies of nanosize dependent metastability of one crystal phase over another.[13] The metastability we refer to, however, is, in a converse way, more similar to the metastability that a non-crystalline bulk structure (*e.g.* an amorphous glass) can possess with respect to a crystalline phase. The size region around N_{meta} denotes the limit at which small nanocrystals start to become structurally unstable and spontaneously relax into non-crystalline species. We note that due to the stability of small clusters often being irregularly dependent on size, it is quite possible that close to size N_{meta} there will be a set of different cluster sizes for which the crystalline order is easier to maintain and sizes for which only non-crystalline clusters are structurally stable.

For the vast majority of materials, neither N_C nor N_{meta} crossover sizes have been determined. For highly ionic materials N_C and N_{meta} will be quite similar and small in magnitude. In other words, in such cases the strong near-isotropic electrostatic interactions between the ions drive the system towards crystalline closely packed structures even for very small sizes (*e.g.* $N < 20$ for $(NaCl)_N$,[14] $(MgO)_N$,[15] $(CeO_2)_N$ [16]). For such materials we note that small to moderately sized crystalline nanoparticles appear to be good theoretical models for calculating the properties of large nanocrystals and/or the corresponding bulk crystal.[17–20] For many materials where the tendency to establish highly ordered atomic arrangements is relatively weaker, we may expect that the N_C and N_{meta} transition sizes could be very different. For example, in such a material one may be able to construct relatively small but very

metastable nanocrystals, but where the thermodynamic NC ↔ C transition occurs at significantly larger nanoparticle sizes. Such a situation has been strongly hinted at in the IP-based studies of $(ZnO)_N$ [21] and $(Fe_2O_3)_N$ [22] nanosystems and is found to be the case in our DFT-based study of the $(TiO_2)_N$ nanosystem. In such cases, calculations using such highly metastable nanocrystal models (*i.e.* with sizes close to N_{meta}) as a means to explain experimental data involving considerably larger nanocrystals and/or bulk crystals, should be very carefully assessed.

Using a bottom-up global optimisation approach we show that, in the case of titania, such small bulk-mimicking nanocrystals are significantly metastable with respect to the most energetically stable nanoclusters of a corresponding size. Furthermore, by also considering a set of bulk-derived nanoparticles for various sizes we estimate the lower size limit at which bulk-like nanoparticles actually start to become the most energetically stable titania species. This latter estimate, corresponding to the N_C size for titania, provides a guide to the size of crystalline nanoparticles which can safely be used as natural stable structural models of larger titania nanoparticles used in the experiment. Generally, our work demonstrates how *ab initio* calculations can provide lower bound estimates for N_C. In other words, we show how the intrinsic size regimes for a material's (nano)crystalline stability can be theoretically predicted.

Methodology

In this study we compare two classes of nanotitania species: (i) nanoclusters derived from bottom-up global optimisation, and (ii) nanocrystals derived from cuts from the anatase bulk phase. As the size ranges covered by these two approaches tend to be quite different, and in order to compare their respective energetic stabilities for arbitrary N, general size dependent relationships between energy and size are required for each class. Below we describe how appropriate relationships were derived in each case. The final reported structures of all nanoclusters, nanocrystals, and the bulk anatase crystal, were fully optimised using DFT calculations with no symmetry constraints employing the PBE0 hybrid functional[23] and a Tier 1/Tight basis set of numeric atom-centred orbitals, as implemented in the all-electron code FHI-AIMS.[24] This level of theory has recently been shown to be good for accurately evaluating both relative total energies and trends in the electronic structure of a range of $(TiO_2)_N$ clusters with sizes between N = 4–20.[25]

Top-down derived $(TiO_2)_N$ nanocrystals

Nanoscale titania, due to its technological importance, is intensively studied both theoretically and experimentally. Ideally, from the computational modelling perspective one would like to employ nanoparticles possessing a realistic size and structure in order to probe their properties using efficient yet acceptably accurate descriptions of their electronic structure. Generally, this entails using calculations based on density functional theory (DFT). Titania nanoparticles used in the experiment, however, typically contain many thousands of atoms; a size that is beyond the current capacity of routine computational modelling using DFT. Efforts to model the optical and electronic properties of nanotitania have thus used a variety of models ranging from nanoclusters containing only a few atoms to nanoparticles possessing up to a few hundred TiO_2 units. Often these studies have attempted to find nanoparticles of titania which retain as much as possible the bulk crystalline and electronic structure. The smallest of these nanocrystals correspond closely to the N_{meta} crossover size below which bulk-like crystallinity cannot be maintained. Nanoparticles as small as $(TiO_2)_{15}$ for rutile[26] and $(TiO_2)_{16}$ for anatase[27] have been reported, and even employed as nanocrystal models.[28] According to our definition of a nanocrystal, we rule out the $(TiO_2)_{16}$ anatase cut as a true nanocrystal due to the large change in atomic positions and accompanying changes in the local bonding of the majority of its atoms that occurs upon relaxing its structure, as also noted in other work.[27]

Herein, we employ five nanocrystals all derived from stoichiometric cuts from the bulk anatase crystal phase with between 28–84 TiO_2 units (*i.e.* 84–252 atoms), which retain their atomic structure reasonably well with respect to the original bulk atomic ordering and positions after structural relaxation (see Fig. 2). Anatase nanocrystals are experimentally

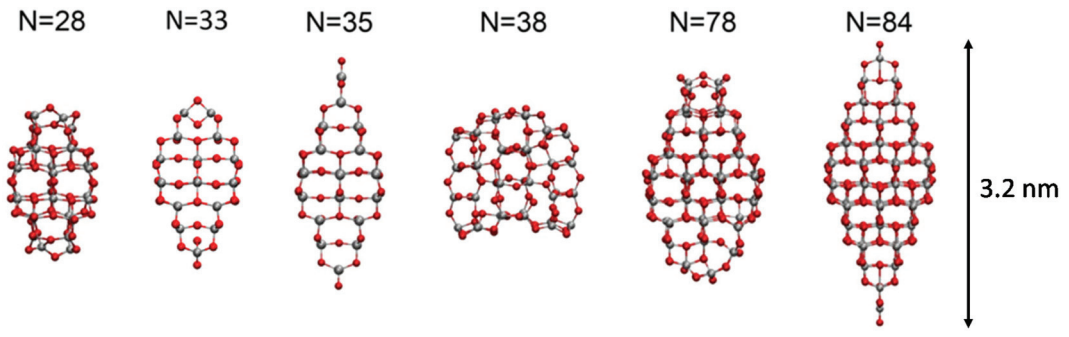

Fig. 2 Atomic structures of the top-down $(TiO_2)_N$ nanocrystals employed. Atom key: O – red, Ti – grey. Note that the scale arrow to the right strictly relates only to the size of the 252 atom $(TiO_2)_{84}$ nanocrystal – the other four nanocrystals have been scaled to show their atomic structure more clearly.

found to exhibit a {101}-faceted bipyramidal shape which typically possess some degree of {001} truncation of the apices. Such a morphology can be rationalised through by cuts of the anatase bulk crystal exposing facets whose size and shape follow their surface energies as described by the Wulff construction.[29] Our nanocrystals with N = 35 and N = 84 were cut from the parent anatase crystal so as to exhibit bipyramidal morphologies, and those with N = 33 and N = 78 units cut to have truncated bipyramidal shapes respectively. The 28 and 38 TiO_2 unit nanocrystals were taken from those studies which used a number of structural principles in order to guide the way in which they were cut from the parent anatase crystal. In particular, the structures of the N = 38 nanocrystal were fabricated according to the requirements that all atoms should have sufficient coordination to support their formal oxidation state (*i.e.* O^{2-} and Ti^{4+} for TiO_2) and that the nanocrystal should have no net dipole moment.[27,30] This procedure results in the N = 38 nanocrystal being fully-coordinated in contrast to the N = 35 and N = 84 bipyramidal nanocrystals which display two apical Ti–O terminations. In the case of the 28 unit nanocrystal a similar, albeit less formal, approach was followed whereby nanocrystals that would be as symmetric as possible in every direction were sought, while still possessing as much anatase-like structure as possible.[31] We note that for this latter $(TiO_2)_{28}$ nanocrystal the original bulk-cut yields four terminal Ti–O groups which persist even after relaxing the structure. Nevertheless, this feature does not appear to detrimentally affect the energetic stability of the nanocrystal compared to similarly sized nanocrystals considered (*i.e.* for sizes N = 33 and N = 35). Conversely, however, we also note that in ref. 31 a N = 38 bulk cut is reported which has two singly coordinated terminal oxygen atoms, which after relaxation form bonds with nearby oxygen atoms (O–O distance of 1.44 Å). This nanoparticle is not used in our study due to this very non-bulk-like feature and the fact that it is highly metastable (>5 eV) relative to the $(TiO_2)_{38}$ bulk cut we employ from ref. 27.

Under the assumption that nanoclusters grow in a perfectly spherical manner one can derive the fraction of surface atoms, $F_{surf}(N)$, to be $kN^{-\alpha}$, where $\alpha = -1/3$ and $k = 4$. Following the derivation for other cluster shapes yields different k values, while α is an unchanged general constant determined by the area-to-volume dimension of $F^{surf}(N)$. Many generic properties, $G(N)$, of simple clusters (*e.g.* total energies, ionisation energies, melting temperatures) can be approximately fitted to a scaling law of the following type:[32]

$$G(N) = G_{bulk} + a_1 N^{-1/3}, \quad (1)$$

where G_{bulk} is a characteristic constant value of the property in question for the chosen bulk phase. For small nanoclusters such fits are worse than those for larger nanoparticles due to the more extreme dependency on properties with small changes in size. This regime of small nanoclusters is often termed the size range where "every atom counts". For large facetted nanocrystals, analysing the most significant size dependent contributions to the total energy yields that it both depends on $F_{surf}(N)$ and $V_{dilate}(N)$, the volume dilation of the nanoparticle induced by surface stress.[3,33] $V_{dilate}(N)$ varies inversely with respect to the radius of the nanocrystal and thus introduces a $bN^{-1/3}$ energy dependence similar to $F_{surf}(N)$. Overall this leads to a general $E(N)$ dependence of the following form for increasingly sized large nanocrystals:[3]

$$\begin{aligned} E(N) &= E_{bulk} + a_1\left(1 - bN^{-1/3}\right)N^{-1/3} \\ &= E_{bulk} + a_1 N^{-1/3} - a_2 N^{-1/3}\cdot N^{-1/3} \\ &= E_{bulk} + a_1 N^{-1/3} - a_2 N^{-2/3}, \end{aligned} \quad (2)$$

where a_1 and a_2 are the constants when the nanocrystals are always of the same shape and crystal structure. We note that for large N, eqn (1) will increasingly become a better approximation to eqn (2) due to the relatively larger magnitude of the exponent of the last term in the latter. More generally, taking eqn (1) as representing the zeroth order dependence on N, we can see eqn (2) as the first three terms of a power series expansion of the form:

$$E(N) = a_0 + a_1 x + a_2 x^2 + a_3 x^3 + \ldots, \quad (3)$$

where $a_0 = E_{bulk}$, $x = N^{-1/3}$ and the a_n values are (possibly N dependent) constants. Eqn (2) has been used to estimate the anatase-to-rutile crossover in titania nanocrystals, with the optimisation of a_1 and a_2 for each polymorph and size considered to obtain the appropriate morphology.[3,34] In this case periodic DFT calculations of bulk titania were used to calculate the surface energies and surface stresses required to evaluate a_1 and a_2.[3] As these top-down calculated values are only strictly valid for infinite slabs, application to faceted nanocrystals was deemed acceptable to the anatase nanocrystals of a minimum size of approximately 450 TiO_2 units (corresponding to a truncated bipyramid with a B/A side length ratio of ~0.3 and side A = 2 nm).[34] Below this size it is more appropriate to perform explicit electronic structure calculations of nanocrystals.[3] In our study we use DFT calculations to directly calculate the fully relaxed structure and energetic stability of $(TiO)_N$ nanoclusters and nanocrystals with sizes $1 < N < 84$ and use these data to extrapolate to nanoparticle sizes with $N \leq 150$. Although quantities calculated for infinite surfaces should not be used in eqn (1) for this size regime, this equation still contains the essential elements to describe the stability of faceted nanocrystals, albeit with more appropriate values of a_1 and a_2.

Bottom-up derived $(TiO_2)_N$ nanoclusters

Numerous previous studies have attempted to find the lowest energy structures of small $(TiO_2)_N$ nanoclusters ($N \leq 20$) without recourse to using bulk crystalline structures.[25,26,35–42] Such a "bottom-up" approach can be attempted by hand using analogy with known nanoclusters of other materials and principles of chemical structure as in ref. 26 and 30. Such intuitive methods, however, are generally not as reliable in finding low energy structures as using global optimisation algorithms to thoroughly search the complex multidimensional potential energy surface (PES) for nanocluster isomer possibilities. The

need for efficient global optimisation tends to increase with nanocluster size as it becomes progressively more difficult to find the lowest energy structures from a bottom-up approach due to the concomitant combinatorial increase in possible atomic configurations.

Here, we employ global optimisation with classical interionic potentials (IPs) to search the PES in a computationally efficient manner, and subsequently refine the resulting low energy cluster structures using unconstrained geometry optimisations at the DFT level of theory. This general IP–DFT strategy has been employed in a number of studies[25,35,39,41,42] with various choices of IP and DFT functionals. We have found that the often-used bulk-parameterised IPs such as those reported by Matsui and Akaogi (MA)[43] are not very size-transferable for evaluating the relative stabilities and structures of small discrete $(TiO_2)_N$ species. We note, for example, that the MA IP tends to predict highly coordinated compact cluster structures to be very energetically stable,[35,42] but which are not found to be particularly low in energy compared to more open structures, when refined using DFT geometry optimizations.[39,41] In an attempt to rectify these shortcomings we have employed two strategies based on the MA IP type.

Firstly, we have taken the original MA IP parameterisation and used this together with another IP which favours the 4-coordination of oxygen ions around each cation. Specifically, we use the interaction parameters of IP by Flikkema and Bromley (FB) which was originally parameterised for $(SiO_2)_N$ nanoclusters.[44] For any particular $(TiO_2)_N$ composition we assign a percentage of the Ti cations and O anions to be treated by the FB IP and the rest by the MA IP. The is purely a formal definition within the overall mixed IP parameterisation and finally all oxygen and all titanium ions are taken to be respectively equivalent after an energy minimisation of a cluster structure. The full set of parameters for this mixed MA–FB IP approach can be found in the ESI.† The FB-treated ions energetically favour the formation of four-coordinated Ti centres largely due to the FB IP possessing a relatively higher degree of O–O repulsion. Thus, when FB-parameterised centres replace the centres originally parametrised by the MA IP (which favour 6-coordinated Ti centres) more open cluster structures are favoured. We found that replacing 30–50% of the original MA-parameterised centres by our FB-parameterised centres was optimal for improving the tendency of the mixed IP to generate low energy $(TiO_2)_N$ cluster structures. We note that this approach was employed previously in ref. 36 to generate candidate global minima for $(TiO_2)_N$ for $N = 8, 10$.

Secondly, we have re-parameterised the original MA IP to reduce its strong tendency to form highly coordinated clusters. Here, the main change was to increase the repulsion between oxygen anions for O–O separations of 1.5–2.5 Å while maintaining very similar Ti–O interaction parameters. We note that the degree of O–O repulsion in this new parameterisation is not as high as in the FB IP (see the ESI† for IP parameters). We found that, as for the mixed IP strategy, this new parameterisation of the MA IP led to low energy cluster structures with relatively less compact structures and fewer highly coordinated Ti centres.

For both the above IP-based approaches we use Monte Carlo basin hopping[45] global optimisation where we typically employ 10 runs each of typically one million steps, each one starting from a different initial structure. For the smallest sizes considered (*i.e.* $N < 15$) we note that the proposed global minima were usually obtained in runs of less than one million steps. During the run, the temperature was automatically adjusted to maintain an average acceptance ratio of new structures of between 65–80%. For the case of the mixed IP approach we also used specific oxygen–oxygen and titanium–titanium swap moves to help ensure that the best configuration of the two oxygen and two titanium types was achieved for any particular cluster structure. The lowest energy 40–50 structures resulting from the 10 runs for each cluster size were then re-optimised using FHI-AIMS with a light Tier 1 basis and the PBE[46] functional. After this refinement, the best 7–8 structures were finally optimised using our reference PBE0/tight Tier 1 settings.

In addition to attempting direct global optimisation of $(TiO_2)_N$ species, we also employed data mining[47] where we took low energy globally optimised structures of $(SiO_2)_N$ [48,49] and $(CeO_2)_N$ [16] and re-optimised them as corresponding $(TiO_2)_N$ nanoclusters. Specifically, we mainly tried columnar-type $(SiO_2)_N$ clusters[49] and tetrahedral $(CeO_2)_N$ fluorite-like cuts.[50] We note, for example, that in the former case low energy structures were found for sizes $N = 12$ and 18, which concurred with the results from our global optimisations. More interestingly, in the latter case, for sizes $N = 10$, 20 and 35, new candidate global minima structures were found as described below.

Results and discussion

For relatively small cluster sizes $(TiO_2)_N$ for $N = 1$–9 we could find no lower energy clusters than those reported previously in the literature indicating that global minima in this size range are reasonably well established. Specifically, our finding for $N = 1$–8 coincide with those reported in both ref. 40 and 41 where global optimisation was performed and, as in the present study, the final structures were optimised with DFT using a hybrid functional. For $N = 9$ and $N = 10$, we concur with the global minima candidate structures found in ref. 41 and 50 respectively. For $(TiO_2)_N$ nanocluster sizes with $N = 11$–14, 16–24, 28, 35 and 38, we report new candidate global minima from our bottom-up global optimisation and data-mining approach (see Fig. 3 and 4). We note that all our reported isomers for these sizes are more energetically stable than any structures we could find in the literature (see the ESI† for a comparison between our results and those reported elsewhere). Herein, we are concerned with the structure and stability of the nanoclusters, and results pertaining to other properties (*e.g.* electronic, vibrational *etc.*) will be reported elsewhere.

In line with the assumptions made in other studies regarding the tendency for higher energetic stability and more bulk-

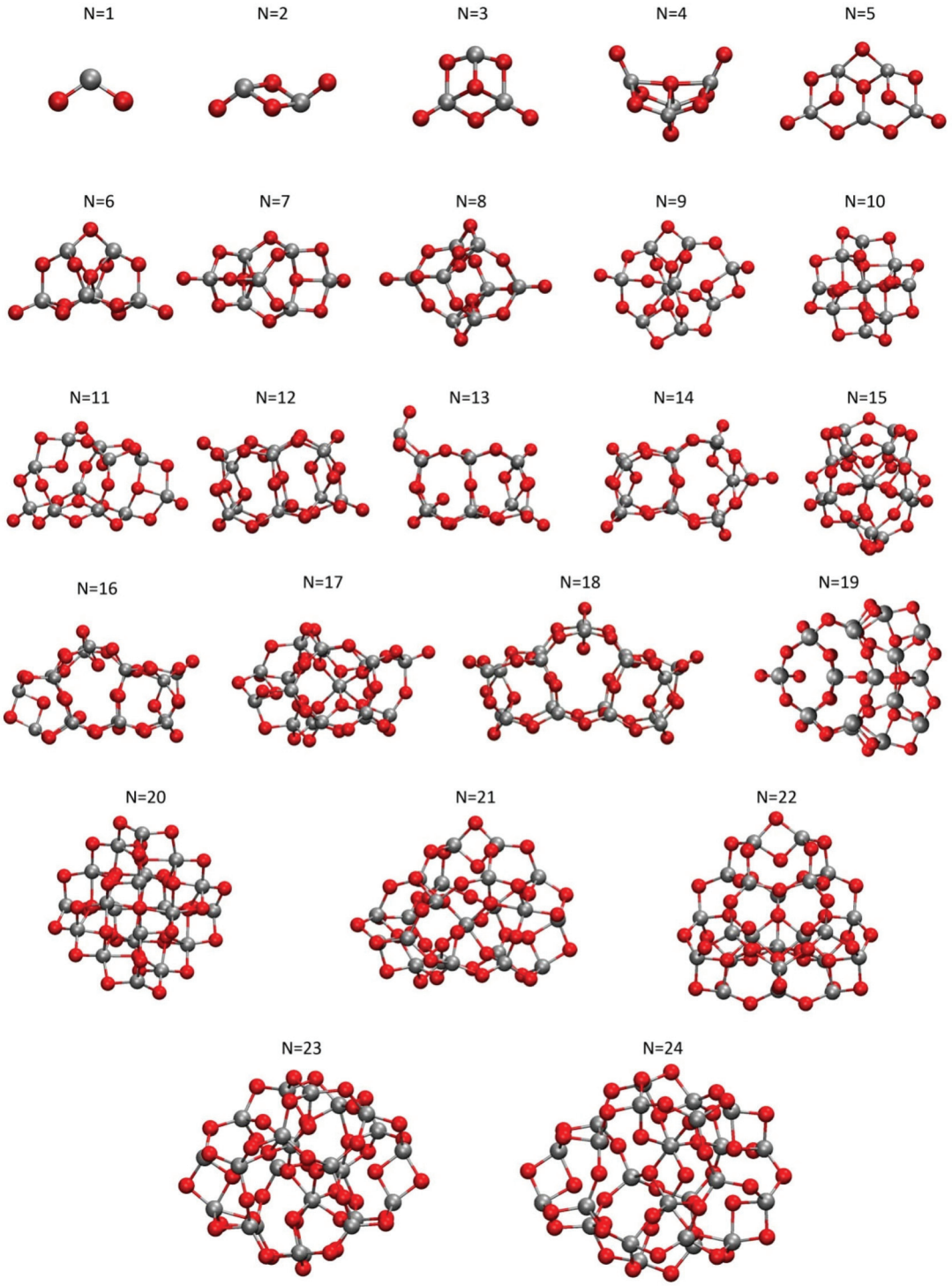

Fig. 3 Structures of the low energy bottom-up derived $(TiO_2)_N$ clusters N = 1–24 employed in this work.

like character being associated with fewer terminal dangling oxygen Ti–O defects,[26,30] our bottom-up generated set of clusters show a clear tendency to exhibit fewer such defects with increasing size. In particular all clusters we find for $N > 18$ are either fully-coordinated (*i.e.* zero terminal defects) or have at most one Ti–O defect. This tendency is also fully in line with the bottom-up studies of $(SiO_2)_N$ clusters where a similar transition to fully-coordinated clusters has been predicted to occur for sizes $N \geq 26$.[51] Generally speaking, we also see a tendency for decreasing structural symmetry in the clusters with increasing size. Although, for example, all $(TiO_2)_N$ global minima in the range N = 1–8 have some symmetry (*i.e.* greater than C_1)

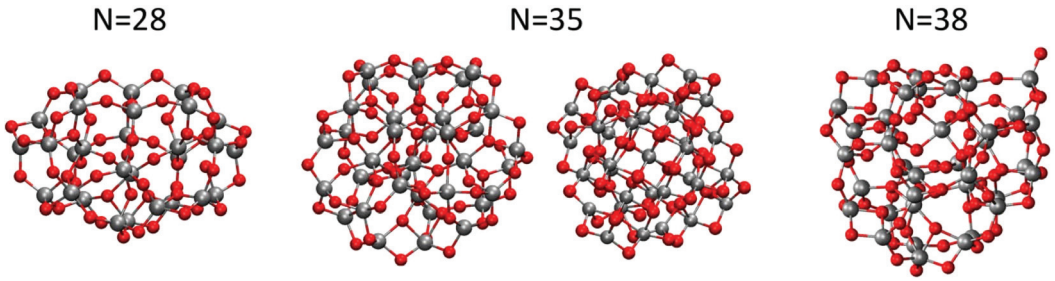

Fig. 4 Structures of low energy bottom-up derived $(TiO_2)_N$ clusters N = 28, 35 (left), 38 found in this work from global optimisation. The N = 35 (right) nanoparticle was obtained from data-mining from a tetrahedral $(CeO_2)_{35}$ nanoparticle in ref. 16 and is calculated to be marginally metastable relative to the $(TiO_2)_{35}$ nanoparticle to its left.

the propensity for our candidate global minima to be symmetric falls away to such an extent that all our lowest energy clusters for $N > 22$ are not symmetric. We note that for the size N = 35, in addition to our lowest energy NC cluster, we also find a highly symmetric and very low energy, yet non-anatase-like, cluster (see Fig. 4) which we discuss below.

Generally, our searches do not find structures which display the anatase crystal structure for N = 1–38. In particular for sizes N = 28, 35 and 38, we find NC clusters which are significantly more stable (by 7.9–9.9 eV total energy) than their correspondingly sized anatase nanocrystal counterparts (shown in Fig. 2). This clearly implies that using metastable anatase nanocrystal structures within this size range to model the behaviour of larger nanocrystals may potentially introduce significant errors, and tests are required to accurately assess the validity and consequences of such modelling approaches.

Estimating the NC ↔ C crossover size regime

Taking the DFT energies of the optimised bulk cut nanocrystals in Fig. 2 we made a fit to eqn (2) to yield a_1 and a_2 for the size range N = 1–150 (see the corresponding data points and blue fit line in Fig. 5). Strictly speaking, as the morphology of our bulk-cut nanocrystals is not always the same, a_1 and a_2 will not be the same for all of them. However, as the considered polymorph (*i.e.* anatase) is always the same and all the considered nanocrystals tend to display similar relaxed surface sites, we fit our eight data points (*i.e.* six bulk cut nanocrystals, and the limits of the infinite anatase crystal and the TiO_2 monomer) with fixed constants for all N values. We also note that by only using the Wulff-type bulk cuts (*i.e.* our bipyramids and truncated bipyramids with N = 33, 35, 78 and 84) we obtain a very similar fit.

For our low energy clusters coming from our bottom-up searches, their structures and morphologies vary immensely with size and thus a fit using eqn (2) is not justified. Instead we assume that although the basic geometric and surface stress energy components of the total energy for regular nanocrystals is captured in eqn (2), a general expansion building on this basis (see eqn (3)) would be more suitable for this diverse set. We have attempted fits using eqn (3) with polynomials from degree 3 to degree 8. We find that for degree 3 and 4 polynomial fits, the resulting extrapolated line does not cross the fit derived for the top-down nanocrystals and simply tends to zero, implying unreasonably, and against experimental evidence, that non-crystalline clusters are always more stable than anatase nanocrystals. For degree 7 and 8 polynomial fits, the extrapolated trend line is non-monotonically decreasing with increasing N, unphysically predicting a decrease in energetic stability with increasing nanoparticle size. Fits with polynomials of degree 5 and 6, however, provide almost exactly the same monotonically decreasing trend line which meets the nanocrystal fit line, which is consistent with the observations. As such, these latter expansions of eqn (3) appear to be the only ones which lead to physical consistent fits of the data. We thus used the degree 5 fit to the nanocluster data which leads to estimate a NC ↔ C crossover size of N = 125 (*i.e.* 375 atoms) as shown in Fig. 5. The fitting parameters used can be found in the ESI† along with the plots of the energetic data with respect to $N^{-1/3}$.

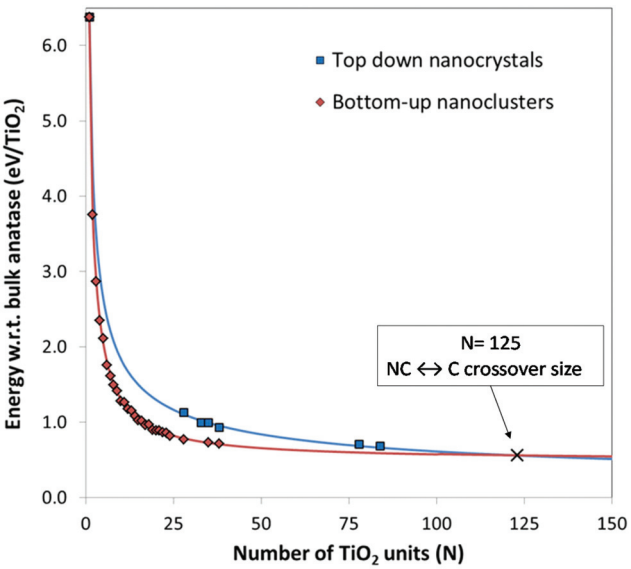

Fig. 5 Energies of bottom-up (red) generated nanoclusters and top-down (blue) generated nanocrystals with corresponding fitting lines. The NC ↔ C crossover size is indicated by a cross at 125 TiO_2 units (*i.e.* 375 atoms).

To provide an idea of the diameter of such an $N = 125$ sized nanoparticle in Fig. 6 we show a spherical semi-crystalline (*i.e.* anatase core and amorphous shell) nanoparticle of 130 TiO_2 units (~2.0 nm diameter) and a facetted anatase bulk cut of 151 TiO_2 units (~2.6 nm diameter). Accordingly, we thus predict the emergence of anatase-like crystallinity in TiO_2 nanoparticle sizes to occur in nanoparticles of approximately 2–3 nm diameter. We note that our prediction, coming purely from a theoretical basis, is fully consistent with the experimental results in ref. 12.

Crystallinity in <2–3 nm diameter non-anatase nanoparticles

Experimentally assessing the degree of crystallinity in very small nanoparticles with diameters <2 nm is clearly complicated by the fact that the concept of long range order is rather ill-defined and thus usual X-ray diffraction (XRD) methods used for larger samples are not applicable. This size regime is also where a bulk electronic structure typically starts to become significantly different from bulk samples also hindering the use of other indirect spectroscopic assessments of bulk-like structures.[52] Theoretically, we can simulate XRD patterns from arbitrarily small nanoparticles but interpreting the results of doing so are rather inconclusive with respect to comparisons with experiment. Here, for example, simulated XRD patterns from seemingly non-crystalline nanoclusters can give rise to broad peaks often taken to be indicative of bulk-like atomic ordering in experimentally measured XRD patterns.[53] To avoid complications of theoretical/experimental comparisons and the formal applicability of XRD for very small nanoparticles, we choose to assess the crystallinity of our nanoparticles through consistently calculating a single alternative measure of the atomic order for both the bulk anatase crystal and our titania nanoparticles. Specifically, we have used the atomic pair distribution function (PDF) which describes the distribution of distances between pairs of atoms in a system (*e.g.* nanoparticle, bulk material). The peaks in the PDF represent the probability to find a neighbourhood particle at the corresponding radial distance from a certain atom. In Fig. 7 we compare the PDFs of a $(TiO_2)_{35}$ top-down bulk cut nanocrystal with that of bulk anatase and the lowest energy $(TiO_2)_{35}$ nanoparticle found from our bottom-up global optimisations. Although clearly not exhibiting the detailed spectra of the perfect bulk anatase crystal, the relaxed top-down $(TiO_2)_{35}$ nanocrystal has a number of well-defined peaks of diminishing size with positions that appear to correspond to those in the bulk anatase crystal. The slight shifting of some peaks to smaller distances in the nanocrystal spectra relative to the bulk anatase spectra is likely due to the surface stress induced compression of the former. Conversely, the more energetically stable bottom-up $(TiO_2)_{35}$ nanocluster has much less well defined spectra with one main fairly broadened peak corresponding to the nearest neighbouring Ti–O bonds. Clearly, although small, the $(TiO_2)_{35}$ nanocrystal can be said to possess some crystallinity, whereas the $(TiO_2)_{35}$ nanocluster is essentially non-crystalline. In this sense, we argue that the blue and red curves, and the point at which they cross in Fig. 5, possess real meaning with respect to a NC ↔ C crossover and thus in assessing the emergence of anatase-like crystallinity with increasing nanoparticle size.

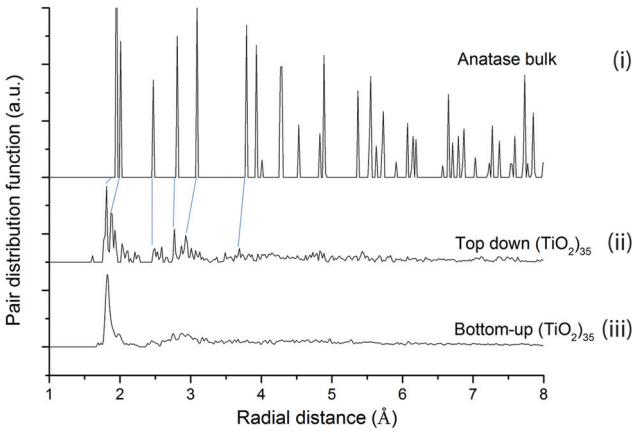

Fig. 7 Pair distribution functions calculated using the Debyer code[54] for: (i) anatase bulk-like nanocrystal, (ii) a top-down $(TiO_2)_{35}$ anatase bulk cut nanocrystal, and (iii) the lowest energy $(TiO_2)_{35}$ nanoparticle from our bottom-up global optimisations. Blue lines indicate tentative correspondence of anatase-like peaks in (i) and (ii).

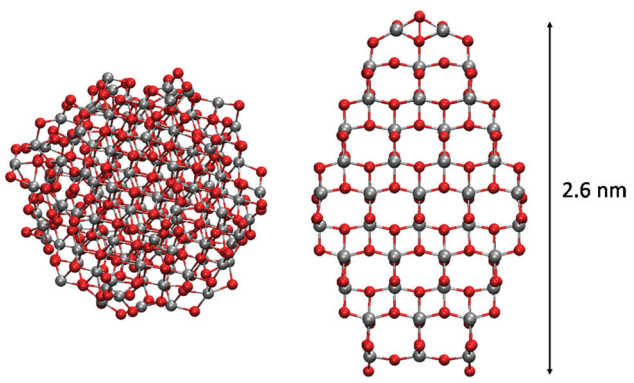

Fig. 6 Nanoparticles with sizes near to the predicted NC ↔ C crossover size. Left: A $(TiO_2)_{130}$ semi-crystalline spherical nanoparticle and right: A $(TiO_2)_{151}$ facetted bulk cut anatase nanocrystal.

Although we have predicted a NC ↔ C crossover which is consistent with experiment, and for which we clearly can define nanocrystals with anatase crystallinity that are metastable to non-crystalline nanoparticles for sizes up to $N = 125$, we also find some very low energy nanoparticles which neither appear to be anatase-like nor totally non-crystalline. Specifically, for $(TiO_2)_N$ sizes $N = 10$, 20 and 35, we obtain very energetically stable nanoclusters from data-mining from tetrahedral nanoclusters reported in ref. 16. For $N = 10$ and $N = 20$ these tetrahedral clusters are actually our best candidate global minima structures. All these nanoclusters are based on cuts from the cubic CeO_2 bulk fluorite crystal structure which has eight-coordinated Ce^{4+} ions and four-coordinated O^{2-} ions. For $(CeO_2)_N$ these bulk-cut-based nanoclusters retain the

as-cut fluorite crystal structure. However, in the case of $(TiO_2)_N$ we find that, upon relaxation, the clusters distort in a such a way as to lower the local atomic coordination of the ions (see the ESI†). This distortion is consistent with the fact that the cubic polymorphs of TiO_2 can only be stabilised at very high temperatures and pressures.[55] Relaxation from a fluorite bulk cut allowing for lowering of coordination would be consistent with a distortion to the columbite crystal structure (*i.e.* the α-PbO_2 structure, also known as the TiO_2 II phase), another known high pressure phase of TiO_2. Experimental X-ray absorption spectroscopy results report evidence for the TiO_2 II phase (*i.e.* columbite) in ~7 nm diameter titania nanoparticles[56] and geologically α-PbO_2-type TiO_2 (*i.e.* columbite) has been found naturally in nanometer sized ultrahigh-pressure inclusions.[57] Indeed, the energetically favoured prevalence for a columbite-like phase at small sizes could be consistent with the high surface stresses in such small nanoparticles which induces an effective high internal pressure. Our comparisons of the structures of the fluorite-cut-derived TiO_2 nanoparticles with the bulk columbite crystal structure, however, do not strongly support the hypothesis that the nanoparticles are simple cuts from the columbite bulk crystal. In fact, although these nanoparticles clearly possess some regular fluorite-derived atomic ordering, they do not appear to be a single phase. From some directions, for example, the clusters appear to exhibit atomic ordering reminiscent of the brookite crystal phase, predicted in some studies to be an intermediate size-dependent stable TiO_2 phase for nanoparticles with diameters between 11–35 nm.[58] The structure of the $Ti_{20}O_{40}$ fluorite-derived nanocluster and its comparison with the original data-mined structure and the brookite crystal can be found in the ESI.†

Conclusions

We present a detailed study of the size dependent energetic stability of nanoscale titania from both a bottom-up and top-down perspective. Using global optimisation and data-mining we report global minima $(TiO_2)_N$ candidates for nanoclusters in the size range N = 1–38 (*i.e.* up to 114 atoms), where in the range N = 11–38, nearly all cluster structures are new and lower in energy than those previously reported. Taking Wulff constructed bulk cuts from the anatase crystal structure and other anatase bulk cuts from the literature, we also track the energetic stability of anatase nanocrystals up to N = 84 (*i.e.* 252 atoms). From direct comparison of the two data sets we can conclude that up to N = 38 anatase nanocrystals are significantly metastable with respect to correspondingly sized non-crystalline nanoclusters. Firstly, this strongly indicates that nanocrystals in this size regime should be employed with caution when used as models of significantly larger nanocrystals and, secondly, that the crossover size at which anatase nanocrystals become more energetically stable than non-crystalline nanoclusters occurs at significantly larger sizes. Using both data sets and fitting using a generalised expansion of a top-down derived energy expression for nanoparticles, we extrapolate the fit to both data sets to predict an approximate NC ↔ C crossover size of N = 125 (*i.e.* 375 atoms). This size corresponds to a nanoparticle diameter of between 2–2.6 nm, depending on nanoparticle morphology, and corresponds well to the observed dominance of amorphous spherical titania nanoparticles of 2–3 nm diameter before facetted anatase nanocrystals tend to take over for larger sizes.[12] We hope that the approach described in this work will inspire similar studies in order to derive estimates of the fundamental NC ↔ C crossover size for a range of other important materials for which nanoscale crystallinity is a key property.

Acknowledgements

Support from Spanish MINECO/FEDER grant CTQ2015-64618-R grant and, in part, by Generalitat de Catalunya grants 2014SGR97, XRQTC is acknowledged. We also acknowledge the NOMAD Center of Excellence project (this project has received funding from the European Union's Horizon 2020 research and innovation programme under grant agreement no. 676580). Access to supercomputer resources was provided through grants from the Red Española de Supercomputación and the COMPHOTOCAT project 2014112608 of the Partnership for Advanced Computing in Europe (PRACE). We also acknowledge funding from H2020 project ITN-EJD-642294 (TCCM: Theoretical Chemistry and Computational Modelling).

References

1 H. Zhang and J. F. Banfield, *Chem. Rev.*, 2014, **114**, 9613–9644.
2 H. Zhang and J. F. Banfield, *J. Mater. Chem.*, 1998, **8**, 2073–2076.
3 A. S. Barnard and P. Zapol, *Phys. Rev. B: Condens. Matter*, 2004, **70**, 235403.
4 X. Chen and A. Selloni, *Chem. Rev.*, 2014, **114**, 9281–9282.
5 M. Kapilashrami, Y. Zhang, Y.-S. Liu, A. Hagfeldt and J. Guo, *Chem. Rev.*, 2014, **114**, 9662–9707.
6 J. Schneider, M. Matsuoka, M. Takeuchi, J. Zhang, Y. Horiuchi, M. Anpo and D. W. Bahnemann, *Chem. Rev.*, 2014, **114**, 9919–9986.
7 W. Dong, Y. Sun, C. W. Lee, W. Hua, X. Lu, Y. Shi, S. Zhang, J. Chen and D. Zhao, *J. Am. Chem. Soc.*, 2007, **129**, 13894–13904.
8 C. Jiang, K. Y. Lee, C. M. A. Parlett, M. K. Bayazit, C. C. Lau, Q. Ruan, S. J. A. Moniz, A. F. Lee and J. Tang, *Appl. Catal., A*, 2016, **521**, 133–139.
9 R. L. Penn and J. F. Banfield, *Geochim. Cosmochim. Acta*, 1999, **63**, 1549–1557.
10 S. Patra, C. Davoisne, H. Bouyanfif, D. Foix and F. Savage, *Sci. Rep.*, 2015, **5**, 10928.
11 J. F. Banfield and H. Zhang, *Mineralogical Society of America*, Washington DC, 2001, vol. 44.

12 H. Zhang, B. Chen, J. F. Banfield and G. A. Waychunas, *Phys. Rev. B: Condens. Matter*, 2008, **74**, 214106–214101.
13 K. Jacobs, J. Wickham and A. P. Alivisatos, *J. Phys. Chem. B*, 2002, **106**, 3759.
14 P. Dugourd, R. R. Hudgins and M. F. Jarrold, *Chem. Phys. Lett.*, 1997, **267**, 186–192.
15 R. Dong, X. Chen, X. Wang and W. Lu, *J. Chem. Phys.*, 2008, **129**, 044705.
16 A. Migani, K. M. Neyman and S. T. Bromley, *Chem. Commun.*, 2012, **48**, 4199–4201.
17 S. T. Bromley, I. Moreira, P. R. de, K. M. Neyman and F. Illas, *Chem. Soc. Rev.*, 2009, **38**, 2657–2670.
18 C. Chizallet, G. Costentin, M. Che, F. Delbecq and P. Sautet, *J. Am. Chem. Soc.*, 2007, **129**, 6442–6452.
19 M. C. C. Wobbe, A. Kerridge and M. A. Zwijnenburg, *Phys. Chem. Chem. Phys.*, 2014, **16**, 22052–22061.
20 C. Loschen, A. Migani, S. T. Bromley, F. Illas and K. M. Neyman, *Phys. Chem. Chem. Phys.*, 2008, **10**, 5730–5738.
21 C. A. C. Richard, S. A. French, A. A. Sokol, A. A. Al-Sunaidi and S. M. Woodley, *J. Comput. Chem.*, 2008, **13**, 2234–2249.
22 A. Erlebach, K. Heinz-Dieter, J. Grabow, F. A. Müller and M. Sierka, *Nanoscale*, 2015, **7**, 2960–2969.
23 C. Adamo and V. Barone, *J. Chem. Phys.*, 1999, **110**, 6158–6169.
24 V. Blum, R. Gehrke, F. Hanke, P. Havu, V. Havu, X. Ren, K. Reuter and M. Scheffler, *Phys. Commun.*, 2009, **180**, 2175–2196.
25 S. Bhattacharya, B. H. Sonin, C. J. Jumonville, L. M. Ghiringhelli and N. Marom, *Phys. Rev. B: Condens. Matter*, 2015, **91**, 241115.
26 Z.-W. Qu and G.-J. Kroes, *J. Phys. Chem. C*, 2007, **111**, 16808–16817.
27 P. Persson, J. C. M. Gebhardt and S. Lunell, *J. Phys. Chem. B*, 2003, **107**, 3336–3339.
28 O. Miroshnichenko, S. Auvinen and M. Alatalo, *Phys. Chem. Chem. Phys.*, 2015, **17**, 5321–5327.
29 G. Wulff, *Z. Kristallogr.*, 1901, **34**, 449–530.
30 P. Persson, R. Bergström and S. Lunell, *J. Phys. Chem. B*, 2000, **104**, 10348.
31 S. Auvinen, M. Alatalo, H. Haario, J.-P. Jalava and R.-J. Lamminmäki, *J. Phys. Chem. C*, 2011, **115**, 8484–8493.
32 R. Johnston, *Masters Series in Physics and Astronomy*, Taylor and Francis, London, 2002.
33 A. S. Barnard and P. Zapol, *J. Chem. Phys.*, 2004, **121**, 4276.
34 A. S. Barnard and L. A. Curtiss, *Nano Lett.*, 2005, **5**, 1261–1266.
35 S. Hamad, C. R. A. Catlow, S. M. Woodley, S. Lago and J. A. Mejias, *J. Phys. Chem. B*, 2005, **109**, 15741–15748.
36 M. Calatayud, L. Maldonado and C. Minot, *J. Phys. Chem. C*, 2008, **112**, 2008.
37 M. Calatayud and C. Minot, *J. Phys. Chem. C*, 2009, **113**, 12186–12194.
38 O. A. Syzgantseva, P. Gonzalez-Navarrete, M. Calatayud, S. Bromley and C. Minot, *J. Phys. Chem. C*, 2011, **115**, 15890–15899.
39 L. Tang, L. Linwei, J. Zhao and R. Qiu, *J. Comput. Chem.*, 2011, **33**, 163.
40 N. Marom, M. Kim and J. R. Chelikowsky, *Phys. Rev. Lett.*, 2012, **108**, 106801.
41 M. Y. Chen and D. A. Dixon, *J. Chem. Theory Comput.*, 2013, **9**, 3189–3200.
42 S. G. Neogi and P. Chaudhury, *J. Comput. Chem.*, 2014, **35**, 51–61.
43 M. Matsui and M. Akaogi, *Mol. Simul.*, 1991, **6**, 239–244.
44 E. Flikkema and S. T. Bromley, *Chem. Phys. Lett.*, 2003, **378**, 622–629.
45 D. J. Wales and J. P. K. Doye, *J. Phys. Chem. A*, 1997, **101**, 5111.
46 J. P. Perdew, K. Burke and M. Ernzerhof, *Phys. Rev. Lett.*, 1996, **77**, 3865–3868.
47 A. Sokol, C. R. A. Catlow, M. Miskufova, S. A. Shevlin, A. A. Al-Sunaidi, A. Walsh and S. M. Woodley, *Phys. Chem. Chem. Phys.*, 2010, **12**, 8438–8445.
48 E. Flikkema and S. T. Bromley, *J. Phys. Chem. B*, 2004, **108**, 9638–9645.
49 S. T. Bromley and E. Flikkema, *Phys. Rev. Lett.*, 2005, **95**, 185505.
50 F. Aguilera-Granja, A. Vega and L. Balbás, *J. Chem. Phys.*, 2016, **144**, 234312.
51 E. Flikkema and S. T. Bromley, *Phys. Rev. B: Condens. Matter*, 2009, **80**, 035402.
52 A. Wood, M. Giersig, M. Hilgendorff, A. Vilas-Campos, L. M. Liz-Marzán and P. Mulvaney, *Aust. J. Chem.*, 2003, **56**, 1051–1057.
53 M. A. Zwijnenburg, *Nanoscale*, 2011, **3**, 3780.
54 Debyer website: https://github.com/wojdyr/debyer. Debyer is a general program for calculating the XRD patterns and pair-distribution functions of nanoparticles.
55 M. Mattensi, J. S. de Almeida, L. Dubrovinsky, N. Dubrovinskaia, B. Johansson and R. Ahuja, *Phys. Rev. B: Condens. Matter*, 2004, **70**, 212101.
56 H. C. Choi, H.-J. Ahn, Y. M. Jung, M. K. Lee, H. J. Shin, S. B. Kim and Y.-E. Sung, *Appl. Spectrosc.*, 2004, **58**, 598.
57 S.-L. Hwang, P. Shen, H.-T. Chu and T.-F. Yui, *Science*, 2000, **288**, 321–324.
58 H. Zhang and J. F. Banfield, *J. Phys. Chem. B*, 2000, **104**, 3481.

